IOP Publishing Semiconductor Science and Technology
Semicond. Sci. Technol. **35** (2020) 085021 (5pp) https://doi.org/10.1088/1361-6641/ab92cf

Fermi level pinning and hydrostatic pressure effect in electron irradiated GaSb

V N Brudnyi[1], I V Kamenskaya[2] and P A Brudnyi[1]

[1] National Research Tomsk State University 36 Lenin av. Tomsk 634050 Russia
[2] Tomsk State Pedagogical University 60A Kievskaya str. Tomsk 634061 Russia

E-mail: Brudnyi@mail.tsu.ru, kamenskayaiv@tspu.edu.ru and paul702 600@gmail.com

Received 20 December 2019, revised 18 April 2020
Accepted for publication 13 May 2020
Published 10 July 2020

Abstract

The effect of 2 MeV electron bombardment up to total electron dose of $1 \times 10^{19} cm^{-2}$ on the electrical and piezo resistive properties of *n*- and *p*-type GaSb crystals was studied. The electron irradiation leads to saturation of the hole concentration at about $5 \times 10^{18} cm^{-3}$ as a result of Fermi level pinning near the valence band top in all irradiated samples. With this in mind, the calculated data on the energy position of the charge neutrality level in GaSb were analyzed. The pressure coefficient of resistivity $\alpha_\rho = \partial(\ln\rho)/\partial P$ was measured as a function of Fermi level position in the electron irradiated samples. Isochronal annealing of radiation-induced defects was investigated in the temperature range of 20–400 $^\circ C$.

Keywords: GaSb, charge neutrality level, radiation effects, piezoresistance

(Some figures may appear in colour only in the online journal)

1. Introduction

Gallium antimonide (GaSb) with a band-gap of 0.73 eV at room temperature (RT) is a suitable material for the manufacture of pressure sensors, infrared detectors, tunnel diodes, broken-gap tunnel field-effect InSb/GaSb transistors, etc. The basic properties of GaSb and the parameters of devices based on it are presented in a number of overviews [1–3]. The problem with this semiconductor is its stable *p*-type ($p = 5 \times 10^{15} - 10^{17} cm^{-3}$) conductivity, regardless of material growing conditions, which represents a major obstacle for practical use of this semiconductor. This feature attributes to the presence in the as-grown crystals of the acceptor-type intrinsic defects, such as Ga vacancies and Ga_{Sb} antisites, in accordance with theoretical calculations and positron annihilation spectroscopy (PAS) measurements [4–9]. In addition to the equilibrium defects, a semiconductor can be over saturated with intrinsic defects as a result of the irradiation with high-energy particles–electrons, ions or fast neutrons. These radiation-induced defects (RIDs) play a significant role in the heavily damaged semiconductor determining its electrical properties.

In the presented work, the change in the electrical properties was investigated in the bulk GaSb crystals after a high-dose of 2 MeV electron irradiation. One of the main goals of this work was to find out the exact Fermi level limit ($F_{\lim}$) position in the irradiated GaSb. This is important since the $F_{\lim}-$value is identical to the charge neutrality level (CNL) position in the energy spectrum of a semiconductor [10]. In turn, the CNL is a universal parameter of the semiconductor the role of which remains a topic of many studies up to date. This level determines not only the electronic properties of the defective crystal, but also the electronic properties of the semiconductor surface and to a large extent the energy diagrams of interfacial stuctures. It is precise with the CNL position in the lower half of the GaSb band-gap associates the stable *p*-type conductivity of this semiconductor [11]. Some studies have been carried out on the electrical properties of the irradiated GaSb crystals earlier, but practically no relevant studies of heavily irradiated material. And although there are a number of experimental studies of the energy spectra of RIDs in GaSb [12, 13], these data to date, are fragmentary, which does not allow to analyze numerically the dose dependencies of the electronic properties of the irradiated samples. Typically, the *p*-type conductivity of

the as-grown GaSb is associated with the presence of an antisite defect Ga_{Sb} with a level near E_V+0.03 eV [6]. The antisites are also typical representatives of RIDs in irradiated semiconductors of III-V group, for example, As_{Ga} in GaAs, P_{Ga} in GaP, etc But irradiated semiconductors have usually fairly rich spectra, therefore, most likely, the pinning of the Fermi level near VBT in irradiated GaSb is determined by the full spectrum of the RIDs.

In current work the effect of the external hydrostatic pressure on the electrical properties in the irradiated samples was examined too. The radiation defects in GaSb under hydrostatic compression have not been studied earlier, despite the unique character of its conduction band structure. These measurements are a particular interest, since being formally a direct-gap semiconductor the GaSb exhibits the properties of an indirect-gap material upon the external hydrostatic pressure due to the energy proximity of the $\Gamma_{6\,C}-$ and $L_{6\,C}-$sub-bands of the conduction band under the normal conditions.

2. Experimental details

The starting materials were the Te—doped *n*-type ($n_0 = 1.56 \times 10^{17} cm^{-3}; n_0 = 2.6 \times 10^{17} cm^{-3}$), undoped *p*-type ($p_0 = 1.91 \times 10^{17} cm^{-3}$) and Zn— doped ($p_0 = 3.3 \times 10^{17} cm^{-3}$) Czochralski's crystals. The as-grown *n*-type crystals were highly compensated and showed a *p*-type conductivity at nitrogen temperatures. Electrical measurements were carried out using Van der Pauw configuration of ohmic contacts. Pure metallic indium was used to contact both *n*- and *p*-type materials, which melted at temperatures of 350–370 $^\circ C$. Prior to metallization and measurements, the native oxide layer was removed by etching in $HF : HNO_3 : H_2O = 1 : 1 : 10$ followed by washing in DI water. The samples with the thickness of 0.6 mm were irradiated with electrons ($E = 2$ MeV, $j = (1–10)\ \mu A/cm^2$) to a total dose of $1 \times 10^{19} cm^{-2}$ using the linear accelerator. In order to avoid irradiation—induced heating the samples during the electron bombardment were kept at liquid-nitrogen temperature. After irradiation the samples were heated up to RT. Isochronal annealing ($\Delta\ t = 10$ min.) of irradiated samples was carried out in organosilicon oil in the temperature range up to 300 $^\circ C$ and in a vacuum at temperatures of 300–400 $^\circ C$. The effect of hydrostatic pressure on the resistivity of initial and electron irradiated samples was measured at RT in the beryllium-copper chamber with silicon oil as a pressure transfer fluid using a calibrated manganin coil enclosed in the bomb.

3. Results and discussion

3.1. Electrical properties

The electrical properties of both initial *n*- and *p*-type conductivity samples are changed after the electron bombardment, but more efficiently in the *n*-type conductivity samples. The dose dependencies of Hall constant (R_H), conductivity (σ) and mobility ($\mu_H = |R_H| \times \sigma$) for initial *n*- and *p*-type conductivity samples, as the result of electron irradiation, are summarized in figures 1(a) and (b) respectively.

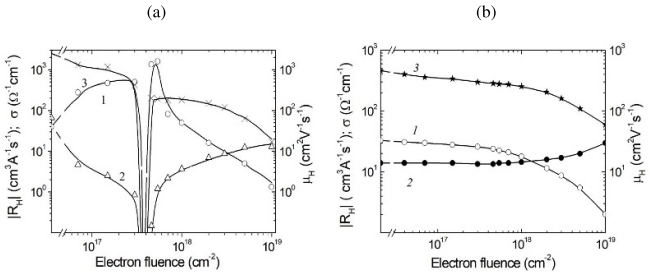

Figure 1. (a) R_H (1), σ (2) and μ_H (3) of initial *n*-GaSb:Te ($n_0 = 1.56 \times 10^{17} cm^{-3}$) vs 2 MeV electrons fluence (RT), (b) R_H (1), σ (2) and μ_H (3) of initial un-doped *p*-GaSb ($p_0 = 1.91 \times 10^{17} cm^{-3}$) vs 2 MeV electrons fluence (RT).

The presented data indicate on the *n*-type activity compensation and on the *n*- to *p*-type conductivity conversion in initial *n*-GaSb samples with an increase of the total electron dose. At the same time, the density of the holes in low doped *p*-GaSb samples increases after the electron bombardment. Upon the high doses of electron irradiation, all studied samples obtained a *p*-type conductivity with a hole concentration at about of $5 \times 10^{18} cm^{-3}$ that corresponds to the Fermi level position near the valence band top (VBT), at about E_V + 0.03 eV. These results close to the previous studies of the proton and neutron-irradiated GaSb samples [14, 15]. At the same time in the initial heavily doped p^+-GaSb:Zn ($p_0 = 1.29 \times 10^{19} cm^{-3}$) samples the concentration of the holes decreases after the proton irradiation which indicates the introduction of the donor-type defects [14]. Thus, the Fermi level upon the irradiation moves into the lower half of the GaSb band-gap and then pinned near the VBT as the result of the self-compensation when the concentration of the charged acceptor-type and donor-type RIDs are close to each other. This *p*-type conductivity of irradiated GaSb is similar to other irradiated III-Sb family semiconductors [10]. The reason of this is an extremely large of valence bands spin–orbit splitting energies in these semiconductors − 0.81 eV (InSb), 0.76 eV (GaSb) and 0.68 eV (AlSb), which leads to a shift of the valence band top in the direction of the CNL by approximately by about of $(1/3)\Delta_{so}$.

3.2. Charge neutrality level

To date, a number of the numerical calculations of CNL value in GaSb have been performed using various analytical models and calculation methods table 1.

The CNL level in these calculations was interpreted as the mid-gap energy averaged at the Γ, X and L special points of the Brillouin zone (BZ) and energy of the model amphoteric deep local state [10], Tersoff's branch-point energy (E_{BP})[16], average sp^3-hybrid energy of f.c.c crystal [17], mid-point energy of dielectric gap [18], reference level of the natural bands alignment in the model-solid [19], E_{BP} – point calculated using the ETB-method [20], Tersoff's E_{BP} – point recalculated using the EMP method [21], reference level from the

Table 1. The calculation data of the CNL position in GaSb with respect to the VBT (eV) from [10, 16–23].

References	[10]	[16]	[17]	[18]	[19]	[20]	[21]	[22]	[23]
ICNL	0.00; 0.14	0.07	0.14	0.06	−0.28	0.16	0.05	−0.07	0.24

valence bands offsets calculations between of III-V semiconductors [22], energy position of the most localized (deepest) model gap state [23]. The calculated data largely depends on the model used and the accuracy of the calculation of the semiconductor energy spectrum. Moreover, these calculations are complicated by high spin–orbit splitting energies of the valence band ($\Delta_{SO} = 0.76$ eV) and $p-d$ coupling in this compound. The results of calculations are listed in the table 1 show a significant scatter of the CNL – values. But these predicted data and their reliability were not sufficiently confirmed by the corresponding experimental measurements. Meantime, the measurement of heavily irradiated semiconductor gives a direct method to obtain the 'experimental' CNL – value as the $F_{\rm lim}$ – position in the energy spectrum of the crystal, since the pinning of the Fermi level is a common phenomenon in irradiated semiconductors [10]. So, using CNL = E_g+0.03 eV gives $\mathrm{CNL}^{abs} = E_g - CNL + EA = 4.76$ eV (RT) in GaSb for electron affinity EA = 4.06 eV, that is close to the work function of GaSb at about 4.76 ± 0.05 eV [24]. The CNL^{abs} – value also is close to the first ionization potential, while the CNL to the surface Fermi level position of GaSb [25].

3.3. Hydrostatic pressure measurements of irradiated GaSb

Hydrostatic pressure is used to divide the so-called shallow and deep local states in the semiconductors. The RIDs (dangling-bond-type defects) exhibit the properties of the deep states since they arise from the extended states of large density of the conduction and valence bands of the crystal. Moreover, for f.c.c. of III-V group semiconductors, the lateral valleys $L_{6\,\mathrm{C}}$ and $X_{6\,\mathrm{C}}$ make the main contribution to the formation of these states. Therefore, the binding energies E_i of these states are pressure sensitive and for low of the external uniform compression P, we can write $E_i(P) \approx E_i(P=0) \pm \gamma_i P$.

Here the pressure coefficients $\gamma_i = \partial E_i/\partial P$ of deep levels contain the information about the energy bands of the crystal, which are involved in the formation of these deep states. To obtain a γ—coefficient, we measured the pressure coefficient of resistivity $\alpha_\rho = \partial(\ln\rho)/\partial P$ as a function of the Fermi level position in the band-gap of the electron irradiated GaSb (figure 2(a)). As shown the α_ρ^n—coefficient of initial n- GaSb samples under the electron irradiation increases to the ultimate value of $3.2\times10^{-4} bar^{-1}$ at an external hydrostatic pressure $P = 5$ $kbar$. Then, after the n-type to p-type conductivity conversion as a result of electron irradiation, the α_ρ—value decreases to $5\times10^{-6} bar^{-1}$, which is close to the corresponding data in the p-type conductivity samples before and after of electron bombardment. These data indicate that RID levels are almost 'tied up' to VBT in GaSb when external hydrostatic pressure is applied.

Taking into account this 'rule of the RID levels pinning' relative to VBT we can write the expression for α_ρ^n—coefficient in the n-GaSb samples as

$$\alpha_\rho^n \approx \partial(\ln\rho)/\partial P = -e\rho\left(\sum_i \mu_i \partial n_i/\partial P + \sum_i n_i \partial\mu_i/\partial P\right). \tag{1}$$

In estimating the α_ρ^n—value we neglected the contribution of the dimensional term since it is small at low pressure. The subscript 'i' in equation (1) denotes the three sub-bands of the GaSb conduction band, which are centered at the $\Gamma_{6\,\mathrm{C}}$-, $L_{6\,\mathrm{C}}$- and $X_{6\,\mathrm{C}}$—symmetry points with separation of 0.084 eV ($L_{6\,\mathrm{C}}$) and 0.31 eV ($X_{6\,\mathrm{C}}$) relative to the $\Gamma_{6\,\mathrm{C}}$-point at the normal conditions. The intersection of these bands under the hydrostatic compression occurs at pressures of about 10 kbar for $\Gamma_{6\,\mathrm{C}} - L_{6\,\mathrm{C}}$, 20 kbar for $\Gamma_{6\,\mathrm{C}} - X_{6\,\mathrm{C}}$ and more than 30 kbar for $L_{6\,\mathrm{C}} - X_{6\,\mathrm{C}}$. The first term in equation (1) describes the change in the electrical resistance of the material due to the redistribution of free electrons between the $\Gamma_{6\,\mathrm{C}}$, $L_{6\,\mathrm{C}}$ and $X_{6\,\mathrm{C}}$ sub-bands under the external hydrostatic compression. The second term in equation (1), takes into account the change in electron mobility at the external hydrostatic pressure, insignificant compared with the first term [26]. In numerical calculations, we neglect by $X_{6\,\mathrm{C}}$ – sub-band, which practically does not affect the electronic properties of lightly doped n-GaSb samples. Therefore, we can write the next relation for the pressure coefficient of resistivity in the n-type samples

$$\alpha_\rho^n \approx \alpha_0/(1+n_1/n_0 b) + \alpha_1/(1+n_0 b/n_1). \tag{2}$$

Here, the subscripts '0' and '1' are denote the parameters of $\Gamma_{6\,\mathrm{C}}$—and $L_{6\,\mathrm{C}}$—sub-bands respectively; while $\alpha_{0(1)} = -\partial(\ln\sigma_{0(1)})/\partial P = \gamma_{0(1)}/kT - \partial(\ln n_{0(1)})/\partial P - \partial(\ln\mu_{0(1)})/\partial P$; $\sigma_{0(1)} = en_{0(1)}\mu_{0(1)}$, $n_0(n_1)$ is the free electron densities in $\Gamma_{6\,\mathrm{C}}$—and $L_{6\,\mathrm{C}}$—sub-bands respectively; $\mu_{0(1)}$ is a corresponding electron mobility and $b = \mu_0/\mu_1$. Neglecting the change in the values of $\mu_{0(1)}$ compared with a change in the density of the free electrons upon the hydrostatic pressure, we can write an approximate expression for estimating of α_ρ^n—value as

$$\alpha_\rho^n \approx \partial(\ln\rho_n)/\partial P \approx -\frac{1}{kT} \times \frac{b\times\gamma_0 + c\times\gamma_1\exp(-\Delta E_{01}(P)/kT)}{b + c\times\exp(-\Delta E_{01}(P)/kT)}. \tag{3}$$

When estimating of the experimental data, the pressure coefficients of the inter-band transitions $\gamma_0 = \partial(\Gamma_{8\,\mathrm{V}} - \Gamma_{6\,\mathrm{C}})/\partial P = 14.2\ meV/kbar$ and $\gamma_1 = \partial(\Gamma_{8\,\mathrm{V}} - L_{6\,\mathrm{C}})/\partial P = 5.4\ meV/kbar$ in GaSb were used [27]. Taking $\Delta E_{01} = (\Gamma_{6\,\mathrm{C}} - L_{6\,\mathrm{C}}) = 0.084\ eV$, $b = \mu_0/\mu_1 \approx 8$ and $c = N_1/N_0 = 50$—the ratio of the density of states in the $\Gamma_{6\,\mathrm{C}}$—and $L_{6\,\mathrm{C}}$ – sub-bands for

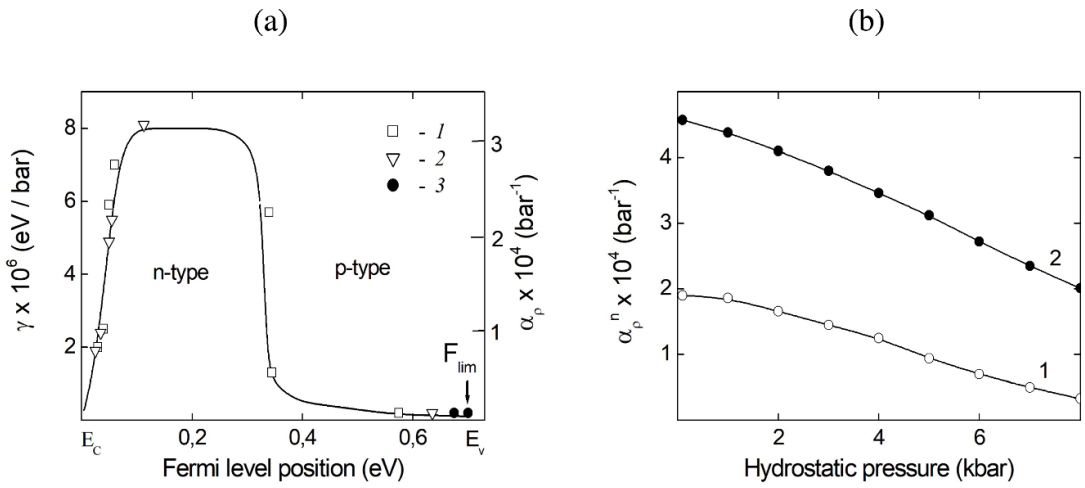

Figure 2. (a) The dependences of γ_i—and α_ρ—coefficients at $P = 5$ kbar vs the Fermi level position in electron irradiated n-type $(1 - n_0 = 1.56 \times 10^{17} cm^{-3}, 2 - n_0 = 2.6 \times 10^{17} cm^{-3})$ and $p - type$ $(3 - p_0 = 3.3 \times 10^{17} cm^{-3})$ GaSb samples (RT), (b) the ultimate values of α_ρ^n- coefficients vs the hydrostatic pressure in initial n-GaSb $(n_0 = 1.56 \times 10^{17} cm^{-3})$ before (1) and after (2) electron irradiation up $D = 1.6 \times 10^{17} cm^{-2}$.

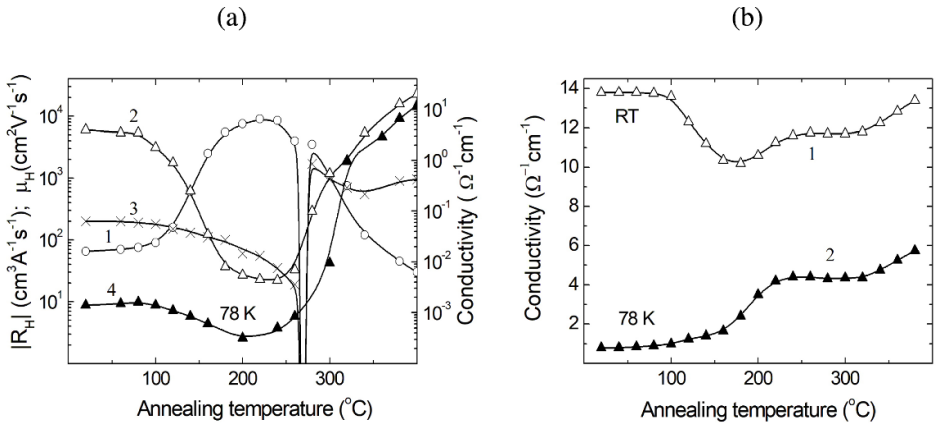

Figure 3. (a) Isochronal (10 min) annealing curves of R_H (1), σ (2) and μ_H (3) at RT and R_H(4) at 78 K in electron irradiated $(D = 1 \times 10^{18} cm^{-2})$ n-GaSb $(n_0 = 1.56 \times 10^{17} cm^{-3})$ samples, (b) isochronal (10 min) annealing curves of σ (RT) and σ (78 K) in electron irradiated $(D = 1 \times 10^{18} cm^{-2})$ p-GaSb $(p_0 = 3.3 \times 10^{17} cm^{-3})$ samples.

$m_0 = 0.041\ m_e^*$ and $m_1 = 0.57\ m_e^*$, where m_e^* is the mass of a free electron, we can estimate the ultimate value of $\alpha_\rho^n \approx 3.4 \times 10^{-4} bar^{-1} (P = 5\ kbar)$ in irradiated n-GaSb samples, which corresponds to $\gamma = 8.9\ meV/kbar$. So, both estimated ultimate values of α_ρ^n and γ are quite close to the experimental data in figure 2(a), taking into account the approximations made. Thus, within the accuracy of the experimental measurements, the RID levels practically don't change their energy positions relative to VBT in GaSb at the external hydrostatic pressure. This asymmetry of pressure coefficients for the RID levels in GaSb is due to the small 'absolute' deformation potential of VBT in comparison with the 'absolute' deformation potential of the conduction band bottom (CBB) in this semiconductor.

Figure 2(b) presents the dose dependencies of ultimate α_ρ^n—pressure coefficients in the initial and electron-irradiated n-GaSb samples as a function of external hydrostatic pressure. In the initial samples, the pressure coefficient decreases with increasing hydrostatic pressure due to the (000) and (111) valleys approaching each other and it tends to zero when all the electrons are completely transferred to the (111) valley. At the same time, the irradiated samples retain significant sensitivity to comprehensive compression over the entire investigated pressure range.

Thus, electron bombardment demonstrates the universal trend, namely, increasing of n-GaSb crystals resistivity, when applying an external compression, with corresponding low sensitivity of irradiated p-GaSb material. This significant improvement in the pressure sensitivity of n-GaSb crystals can be used in the design of hydrostatic compression sensors. At the same time, in contrast to the pressure sensors on the material doped with deep chemical impurities Fe, Co, Ni and so on, the irradiation is a well-controlled manufacturing process for such sensors.

3.4. Post-irradiation isochronal annealing

Isochronal annealing of irradiated samples was fulfilled up to 400 °*C*, since at higher temperatures of the thermal treatment the electronic properties of original samples are changing too [28, 29]. The isochronal curves of R_H, σ and $\mu_H = \mid R_H \mid \times \sigma$ in the heavily irradiated initial *n*- and *p*-type samples are presented in figures 3(a) and (b).

These data show a 'reverse' transition from *p*-type conductivity in the heavily irradiated samples to its initial *n*-type conductivity state upon the heating at the temperatures higher than 250 °*C*. Wherein, at 400°*C* the R_H is almost restored to its initial value, while, at the same time, the electron conductivity is restored partially. From figure 3(a) it is visible that R_H (78 K) too almost completely restored out at 400°*C* (before irradiation the initial *n*-GaSb (RT) samples had a *p*-type ($p \approx 10^{14} cm^{-3}$) conductivity near 78 K). Isochronous annealing curve R_H (78 K) demonstrates an annealing of donor-type defects in the temperature range of 100–200 °*C*. In the heavily irradiated initial *p*-GaSb samples the R_H value is practically restored at 400 °*C* too, while the conductivity is partially only. Annealing curves of σ (RT) demonstrate the annealing of acceptor-type defects at temperatures of 100–180 °*C* and donor-types at 180–250 °*C* and above 300 °*C*, while σ (78 K)—curves indicate the annealing of donor-type defects at temperatures of 100–230 °*C* and above 300 °*C*. Thus, in heavily electron-irradiated GaSb samples after the thermal heating up to 400 °*C* there are the residual RIDs. It is possible that these defects in the partially annealed out samples are the secondary defects which are formed upon an irradiation or post-irradiation annealing due to migration of the primary point defects. For example, the bombardment of GaSb with 2 MeV electrons near liquid-nitrogen temperature leads to the formation of the dislocation loops of interstitial-type as a result of the interstitial atoms fast migration [30].

4. Summary

The initial *n*- and *p*-type conductivity crystals of GaSb after electron, proton or neutron irradiation acquire a non-degenerated *p*-type conductivity with a Fermi level pinning position almost near VBT. The *p*-type conductivity is characteristic to all of III-Sb irradiated semiconductors as a result of significant spin–orbit splitting energies of their valence bands, which leads to a decrease in the energy gap between CNL level and valence band top in these semiconductors. It should be noted that surface layers of the GaSb with various types of its bulk conductivity have the *p*-type conductivity too, i.e. in highly irradiated samples the model of the flat zones (zero surface potential) is realized. When the external hydrostatic pressure is applied, the RID's levels in GaSb shift down from the conduction band bottom, while at the same time, ones are quite fixed relative to the valence band top as the result of the strong asymmetry of absolute deformation potentials of the VBT and CBB in this semiconductor.

Acknowledgment

This work was supported by the Ministry of Education and Science of the Russian Federation (Project # 3.7660.2017/6.7) and by the National Research Tomsk State University Academic D.I. Mendeleev Fund Program.

ORCID iDs

V N Brudnyi https://orcid.org/0000-0001-5697-2173
P A Brudnyi https://orcid.org/0000-0002-9579-5971

References

[1] Dutta P S, Bhat H L and Kumar V 1997 *J. Appl. Phys.* **81** 5821–70
[2] Vurgaftman I, Meyer J R and Ram-Mohan L R 2001 *J. Appl. Phys.* **89** 5815–75
[3] Bennet B, Magno R and Boos J B *et al* 2005 *Solid-State Electron* **49** 1875–1895
[4] Kujala J, Segercrantz N A, Tuomisto F and Slotte J 2014 *J. Appl. Phys.* **117** 143508
[5] Virkkala V, Havu V, Tuomisto F and Puska M J 2012 *Phys. Rev.* B **86** 144101
[6] Ling C C, Lui M R and Ma S K *et al* 2004 *Appl. Phys. Lett.* **85** 384–88
[7] Chroneos A and Bracht H 2008 *J. Appl. Phys.* **104** 093714
[8] Hakala M, Puska M J and Nieminen R M 2002 *J. Appl. Phys.* **91** 4988–94
[9] Hui L, Kai Z and Jingbiao P 2011 *Semicond. Sci. Technol.* **26** 075016
[10] Brudnyi V N, Grinyaev S N and Stepanov V E 1995 *Physica* **212** 429–35
[11] Segercrantz N, Slotte J and Tuomisto F *et al* 2017 *Phys. Rev.* B **95** 184103
[12] Murawala P A, Arora B M and Chandvankar S S 1986 *Sci. Forum Mater.* **10–12** K139–42
[13] Nakashima K 1987 *Jpn. J. Appl. Phys.* **26** 423–27
[14] Brudnyi V N and Kamenskaya I V 1988 *Phys. Status Solidi* a **105** K141–44
[15] Boiko V M, Brudnyi V N, Ermakov V S and Kolin N G *et al* 2015 *Semiconductors* **49** 763–66
[16] Tersoff J 1986 *J. Vac. Sci. Technol.* B **4** 1065
[17] Harrison W A and Tersoff J 1986 *J. Vac. Sci. Technol.*B **4** 1068–75
[18] Cardona M and Christensen N E 1987 *Phys. Rev.* B **35** 6182–94
[19] Van C G and Neugebauer J 2003 *Lett. Nat.* **425** 626–28
[20] Monch W 1996 *J. Appl. Phys.* **80** 5076–82
[21] Brudnyi V N and Grinyaev S N 1998 *Semiconductors* **32** 284–87
[22] Wie S H and Zunger A 1998 *Appl. Phys. Lett.* **72** 2011–13
[23] Brudnyi V N, Grinyaev S N and Kolin N G 2003 *Semiconductors* **37** 557–64
[24] Gobeli G W and Allen F G 1965 *Phys. Rev.* A **137** 245–54
[25] Sidor D E, Savich G R and Wicks G W 2015 *Proc. SPIE V.9616. Nanophot. and Macrophot. for Space Environments IX* (San Diego, US)
[26] Paul W and Warschauer D M 1963 *Solids Under Pressure* (New York: McGraw-Hill)
[27] Wei S H and Zunger A 1999 *Phys. Rev.* B **60** 5404–11
[28] Su J, Liu T, and Liu J M *et al* 2016 *Chin. Phys.* B **25** 077801–9
[29] Su J, Liu T and Liu J *et al* 2017 *J. Semicond* **38** 043001
[30] Nitta N, Taguchi E and Yasuda H *et al* 2011 *Phil. Mag. Lett.* **91** 223–38